

# Low insulin content of large islet population is present in situ and in isolated islets

Han-Hung Huang, Lesya Novikova, S. Janette Williams, Irina V. Smirnova and Lisa Stehno-Bittel\*

Department of Physical Therapy and Rehabilitation Science; University of Kansas Medical Center; Kansas City, KS USA

**Key words:** Islet,  $\beta$ -cell, insulin, rat, islet isolation, electron microscopy

**Abbreviations:** BSA, bovine serum albumin; DAPI, 4',6-diamidino-2-phenylindole; EDTA, ethylenediaminetetraacetic acid; ELISA, enzyme-linked immunosorbent assay; FBS, fetal bovine serum; IHC, immunohistochemistry; IE, islet equivalents; PBS, phosphate buffered saline; SCB, sodium cacodylate buffer; TEM, transmission electron microscopy

The existence of morphologically distinct populations of islets in the pancreas was described over 60 years ago. Unfortunately, little attention has been paid to possible functional differences between islet subpopulations until recently. We demonstrated that one population, the small islets, were superior to large islets in a number of functional aspects. However, that work did not determine whether these differences were inherent, or whether they arose because of the challenge of isolation procedures. Nor, was there data to explain the differences in insulin secretion. We utilized immunohistochemistry, immunofluorescence, ELISA and transmission electron microscopy to compare the unique characteristics found in isolated rat islet populations in situ and after isolation. Insulin secretion of small isolated islets was significantly higher compared to large islets, which correlated with higher insulin content/area in small islets (in situ), a higher density of insulin secretory granules and greater insulin content/volume in isolated islets. Specifically, the core  $\beta$ -cells of the large islets contained less insulin/cell with a lower insulin granule density than peripheral  $\beta$ -cells. When insulin secretion was normalized for total insulin content, large and small islets released the same percentage of total insulin. Small islets had a higher density of cells/area than large islets in vitro and in situ. The data provide a possible explanation for the inferior insulin secretion from large islets, as they have a lower total cell density and the  $\beta$ -cells of the core contain less insulin/cell.

## Introduction

Morphometrical analysis, first reported in 1947, showed differences in size distribution, number and volume of islets from several species<sup>1-7</sup> including human.<sup>8-12</sup> In spite of morphological analysis showing distinct populations of islets, most researchers and clinicians still consider all islets to be functionally equivalent.

It is surprising that many details about the function of islets are still unknown.<sup>11,13</sup> In 2001, an important paper examined the functional differences between islets that related to their size.<sup>3</sup> The authors showed a variety of functionally different islet characteristics, including the fact that 60% of the islets responded to glucose challenge with a dose-dependent insulin release, versus 32% of islets that had an all-or-none response. Other structural variations based on islet size were published recently.<sup>9</sup>

Our laboratory reported that isolated small islets from rats were superior to large islets in function and in transplantation outcomes, especially when measuring insulin secretion.<sup>14</sup> Subsequent experiments by other laboratories confirmed similar results in human and mouse islets.<sup>15,16</sup> To further characterize these differences, we determined that large islets contained a significant diffusion barrier that hampered viability of the islets

in culture.<sup>17</sup> Surprisingly, elimination of the diffusion barrier in large rat islets did not restore insulin secretion to the same rate as intact small islets, suggesting that there were inherent cellular differences between large and small islets<sup>17</sup> which might explain the inferior insulin secretion by the cells within the large islets.

The behavior of islets in culture has important implications for islet transplantation. Yet a more important question lingers; are these differences in islet function solely a result of the ability of islets of different sizes to withstand the isolation procedure, or do these functional differences exist in vivo? The experiments described in this paper begin to elucidate the morphological and functional differences in rat islet subpopulations, and to determine whether these differences exist prior to isolation.

## Results

**Insulin secretion.** Perfusion experiments illustrated that under basal conditions, and at each time point of the biphasic response, the small islets released more insulin per volume (islet equivalent; IE) than large islets. **Figure 1** shows the results of the enzyme linked immunosorbent assay (ELISA) from approximately 1,400 islets from six rats. While similar results have been published

\*Correspondence to: Lisa Stehno-Bittel; Email: lbittel@kumc.edu  
Submitted: 08/31/10; Revised: 10/29/10; Accepted: 11/05/10  
DOI: 10.4161/isl.3.1.14132

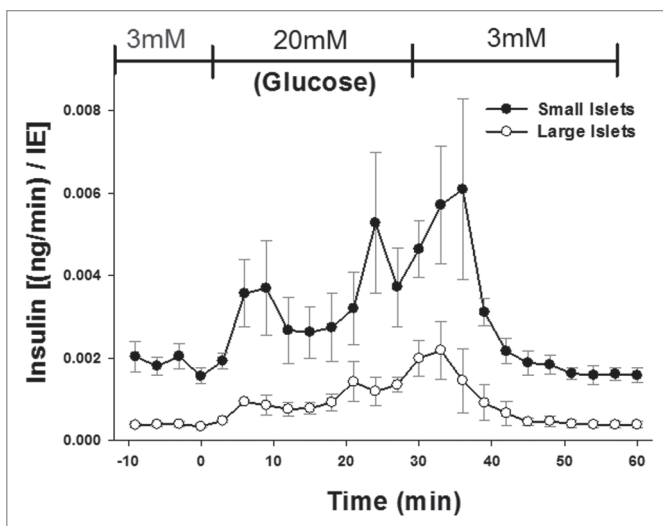


**Figure 1.** Small isolated islets secrete more insulin per volume. Isolated islets were separated into large and small populations and exposed to low and high glucose (indicated at top of graph). At each time point more insulin was released by the small islets than the large ( $p < 0.001$ ).

previously with human islets,<sup>15</sup> the rationale given for the difference in insulin secretion between large and small islets has been attributed to core cell death in the large isolated islets.<sup>14</sup> Our previous publication indicated that such an explanation was insufficient to account for the dramatic differences in insulin secretion from large islets.<sup>17</sup> Thus, we designed a series of experiments to determine whether there existed inherent differences in large and small islets prior to isolation that could account for the different insulin secretion rates.

**Islet cell composition.** The first hypothesis to be tested was that small islets contained a higher percentage of  $\beta$ -cells than large islets and this accounted for the higher insulin secretion. Using immunofluorescently-stained serial sections of the pancreas, the islet cell composition was analyzed (Fig. 2A and B). In order to critically classify the islet as large or small, serial sections of 10  $\mu\text{m}$  were obtained and only sections with the greatest islet diameter were analyzed. Approximately 60% of the endocrine cells were composed of  $\beta$ -cells in large and small islets in situ (Table 1).

The cellular make-up of the large and small islets was analyzed after isolation (Fig. 2C and D). Again, 65–69% of the stained cells were  $\beta$ -cells (Table 1). The isolated large islets had a higher proportion of  $\alpha$ -cells than isolated small islets, but the difference was minor and did not appear to be enough to alter the total insulin secreted from this population of islets (Table 1). Unlike humans, the rat islet architecture is organized with  $\alpha$  and  $\delta$ -cells localized to the periphery, while  $\beta$ -cells were predominantly found in the center of the islet. In the large islets, three to four layers of  $\alpha$ - or  $\delta$ -cells were located at the periphery in situ (Fig. 2A and B). There was a clear loss of the peripheral  $\alpha$ - and  $\delta$ -cells after isolation (Fig. 2C and D). This loss of peripheral cells was likely due to the isolation process, in agreement with the results of others.<sup>24,25</sup>

One limitation with the analysis of serial sections is that it is possible to miss or over-count certain cell types, because of the

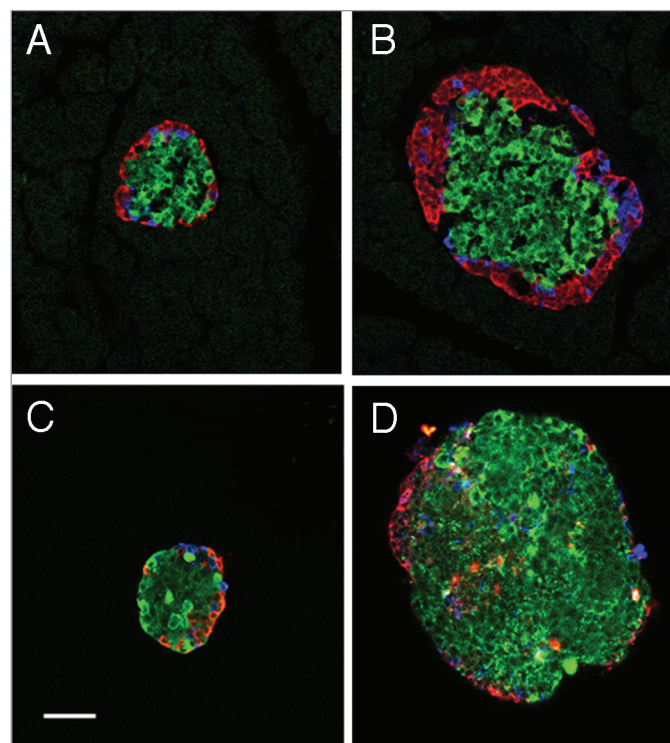


**Figure 2.** Cellular composition does not differ with islet population. Islets were immuno-fluorescently labeled for  $\beta$ -cells (insulin = green),  $\alpha$ -cells (glucagon = red) and  $\delta$ -cells (somatostatin = blue). Small (A) and large (B) islets labeled within pancreatic sections (in situ) show same general cell composition. Small (C) and large (D) islets after isolation also have the same general composition. Loss of peripheral  $\alpha$ - and  $\delta$ -cells was noted in the isolated islets (C and D) compared to in situ (A and B). (Scale bar = 50  $\mu\text{m}$  for all images).

2D properties of the preparation. To overcome this limitation, we repeated the experiments using islets from the two populations dissociated into single cells and labeled for cell types. The results show that there was no significant difference in the proportions of  $\beta$ -cells to other endocrine cells between small and large islets (Table 1). Finally, we co-stained isolated islets with insulin antibodies (to identify  $\beta$ -cells) and DAPI (to stain nuclei, providing a total cell count). There was no significant difference in the proportion of  $\beta$ -cells to total islet cells between small (47%) and large (50%) islets. Thus, the first hypothesis of a greater proportion of  $\beta$ -cells in small compared to large islets proved to be false.

**Islet cell density.** While the proportion of  $\alpha$ -,  $\beta$ - and  $\delta$ -cells within islets from the two populations was not different, we hypothesized that the total cell density might be greater in small islets, leading to a higher total number of  $\beta$ -cells per small islet volume. Immunofluorescence of islets in pancreatic sections and after isolation showed that small islets consistently had a higher endocrine ( $\alpha$ -,  $\beta$ - and  $\delta$ -cells) cell density that was significantly greater than large islets (Fig. 3A). Isolated small and large islets viewed with transmission electron microscopy (TEM) illustrated a higher total cell density in small islets compared to large (Fig. 3B).

As described above, the inherent limitations when counting cells within a 2D image required that we verify the results with a third method. Thus, we isolated 293 islets with diameters of

**Table 1.** The proportion of  $\alpha$ -,  $\beta$ - and  $\delta$ -cells in small and large islets were compared in isolated intact islets (in vitro, intact), isolated islets dissociated into single cells (in vitro, dissociated), and in pancreatic sections (in situ)

	Small Islets (% of endocrine cells)			Large Islets (% of endocrine cells)		
	$\beta$ -cells	$\alpha$ -cells	$\delta$ -cells	$\beta$ -cells	$\alpha$ -cells	$\delta$ -cells
<b>In situ</b>	59	25	16	61	29	10*
<b>In vitro (intact)</b>	69	19	12	65	24*	11
<b>In vitro (dissociated)</b>	74	17	9	70	24*	6

\*Indicates a statistically significant difference for the individual cell type between large and small islets;  $p < 0.05$ .

either 50 or 200  $\mu\text{m}$ . The islets were dispersed into single cells, and the number of cells/islet counted. Using this method, the total cell count per volume was recorded. The density of cells was calculated as the total number of cells/volume (IE) of the original islets (Table 2). Again, the results demonstrate that the total number of cells/volume of islets was greater in the small than large islets. In summary, immunofluorescence (in situ and in vitro), calculations from TEM micrographs (in vitro) and the counting of dispersed cells all agreed that the small islets had a higher cell density.

**Insulin content.** With a greater total cell density in the small islets, we hypothesized that the insulin content stored within individual  $\beta$ -cells could be greater in cells from small compared to large islets. To test this hypothesis, we utilized three approaches; the density of insulin granules from isolated islets was calculated from TEM, the total insulin content of isolated islets was determined by ELISA, and the in situ insulin content per islet and per cell was calculated with immunohistochemistry.

The mean insulin granule density (granules/area) was calculated from  $\beta$ -cells within large and small islets. Figure 4 illustrates the differences in granule density between small (A) and large (B) islets. There was a statistically significant increase in the average density of insulin granules in the small islets compared to large islets (Fig. 4C). Our granule counts are consistent with published figures using the same methods.<sup>26</sup>

Further confirmation was obtained by analyzing the total intracellular insulin content of isolated islets. Again, more total insulin per volume (IE) was measured in small compared to the large islets under both basal conditions (low glucose) and following a 30 min in vitro high glucose exposure (Fig. 4D). To test insulin content in situ, pancreatic sections were stained for insulin and the intensity of the immunohistochemistry stain/islet was quantified. Once more, the insulin content was greater in the small islets (Fig. 4E). Thus, using three independent approaches from both in situ and in vitro preparations, evidence supported the hypothesis that small islets contain more insulin per volume or area than large islets.

Interestingly, normalization of the glucose-stimulated insulin release as a percentage of the total insulin content of the islets demonstrated that large and small islets actually secreted the same percentage of their total insulin content over time (Fig. 4F). The difference in absolute insulin secretion levels was not likely due to secretory mechanisms, but rather in the increased insulin stored within the  $\beta$ -cells of the small islets.

**Insulin location.** Immunohistochemistry demonstrated a stark difference in the intensity of insulin staining depending on

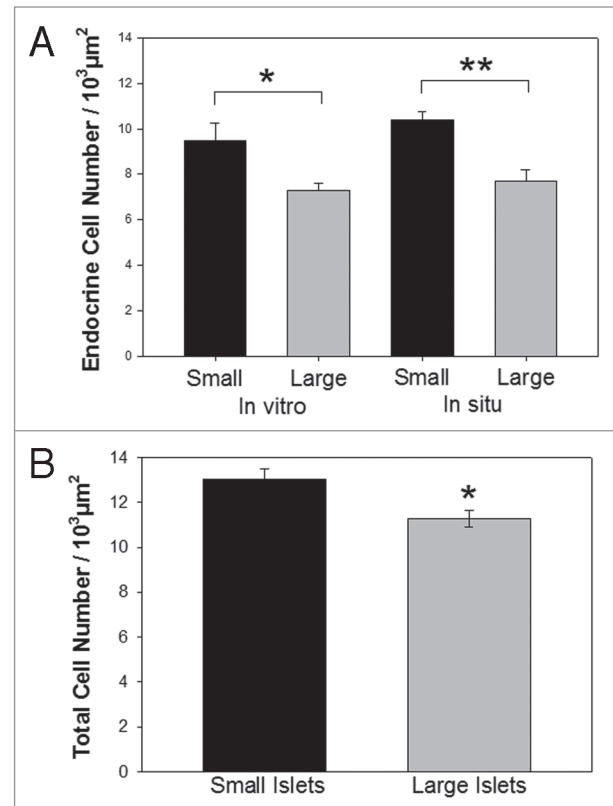


**Figure 3.** Cell density higher in small islets. (A) The density of  $\alpha$ ,  $\beta$  and  $\delta$ -cells within small and large islets were calculated as cells/area from immunofluorescent images of pancreatic sections (in situ) and from isolated islets (in vitro). (B) The total cellular density was measured from TEM micrographs of isolated islets. (\* $p < 0.05$ ) and (\*\* $p < 0.01$ ).

**Table 2.** The number of cells dissociated from small or large islets were counted and calculated as cells/volume (IE)

Islet Diameter ( $\mu\text{m}$ )	Cells per islet (mean $\pm$ SE)	Cells/IE
Small (50 $\mu\text{m}$ )	83 $\pm$ 22	2235
Large (200 $\mu\text{m}$ )	2071 $\pm$ 75	874**

\*\*Small islets contain significantly more cells per volume than large islets ( $p < 0.001$ ).

the location of the  $\beta$ -cell in the islet. We analyzed the intensity of the insulin immunostaining per cell within the islets. In small islets all  $\beta$ -cells contained approximately the same level of insulin staining (Fig. 5A). In large islets, insulin-containing  $\beta$ -cells located at the periphery of the islets contained approximately

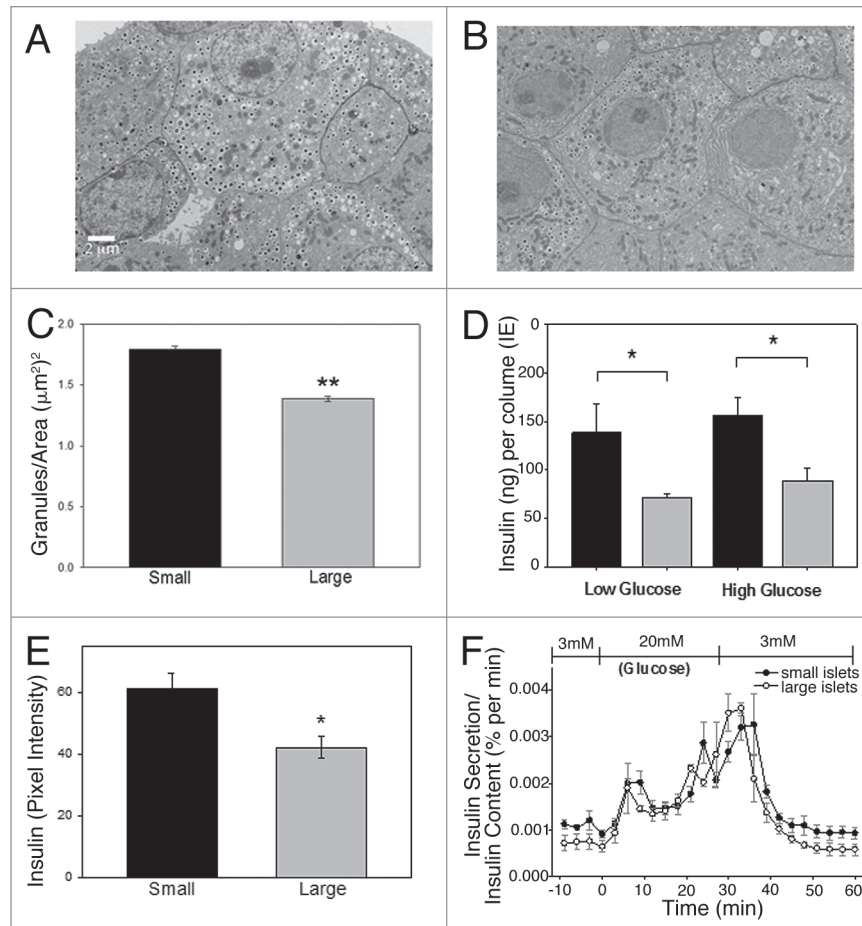


**Figure 4.** Small islets have greater insulin content than large islets. (A) Typical TEM micrograph showing  $\beta$ -cells from small islet with densely packed insulin granules. (B) Typical  $\beta$ -cells from large islet with fewer insulin granules. Scale bar = 2  $\mu\text{m}$  for images (A and B). (C)  $\beta$ -cells from isolated small islets have a greater density of insulin granules than  $\beta$ -cells from large islets ( $p < 0.001$ ). (D) Total insulin content from small (black bars) and large (gray bars). Isolated islets (measured by ELISA) showed that small islets, in low or high glucose, contained more insulin per volume ( $p < 0.05$ ). (E) Insulin labeling intensity of islets in situ also demonstrated higher values for  $\beta$ -cells from the small islets compared to large islets ( $p < 0.05$ ). (F) After normalizing insulin secretion to total insulin content/islet, there was no statistical difference in the level or timing of the first or second phase insulin secretion amount between large and small islets.

the same level of insulin per cell as those within the small islets (Fig. 5B). However,  $\beta$ -cells located within the core of the large islets contained significantly less insulin per area (Fig. 5B and C). This observation was extremely reproducible with 100% of the examined large islets illustrating the insulin-prominent outer layer of cells. Due to the inherent variation in staining intensity, comparisons were made within preparations. Figure 5C shows the results from one animal, but is representative of three independent replications. Because these findings had not been reported previously, we undertook a series of experiments to confirm the results. We stained serial sections of the pancreas for insulin using a 3-amino-9-ethyl-carbazole or a 3,3'-diaminobenzidine chromogen substrate to visualize staining. Both resulted in less insulin staining in the core cells of the large islets. Subsequently, we repeated the experiments using three different insulin antibody dilutions (1:50, 1:100 and 1:200) to be sure that the lighter insulin staining in the core was not an artifact of the procedures. With all three dilutions, the results were the same; the insulin staining of the core cells within the large islets was less compared to the periphery

and compared to the cells of small islets. The same characteristic, low insulin-containing  $\beta$ -cells in the core of large islets, was noted in isolated islets in culture. In large islets, insulin-secreting  $\beta$ -cells located at the periphery of the islets contained more insulin than the cells located within the central core (results not shown).

TEM analysis of the insulin-containing vesicles in  $\beta$ -cells from the core of the large isolated islets compared to the periphery supported the immunohistochemistry results. Figure 6A and B illustrate typical sections from the core (A) and periphery (B) of a large islet. The density of secretory granules was calculated by counting the number of granules/defined area and the results are shown in Figure 6C. There were statistically more secretory granules in the  $\beta$ -cells of the peripheral cells when compared to the core cells of the large islets. Thus, the differences in intracellular insulin content between large and small islets appears to be at least partially due to a lower amount of insulin in the  $\beta$ -cells within the core of the large islets.

**Characteristics of core  $\beta$ -cells in situ.** Because most explanations concerning the functional differences between large and

small islets focus on the core cell death found in isolated large islets, and we identified inferior insulin content in large islets in situ, we examined the general characteristics of the core  $\beta$ -cells within the large islets using TEM. Using previously published methods to quantify the quality of mitochondria with electron micrographs,<sup>23</sup> we determined that 92% of the mitochondria from  $\beta$ -cells of large islets were completely intact (grade 1) with the remaining 8% scored as grade 2 (<50% disruption of inner mitochondrial membrane). No mitochondria from  $\beta$ -cells within large or small islets contained compromised mitochondria (grade 3–5). There was no difference in the mitochondrial scores for the cells from large or small islets. Thus, cell damage during tissue processing could not explain the poor insulin staining in the core of the large islets.

## Discussion

In 1979, Baeten et al. described different islet architecture associated with islets located in regions of exocrine tissue that drained into different ducts.<sup>10</sup> They concluded that their research contradicted the widely-held belief that all islets have similar composition. Since that time, numerous labs have extended the description of morphological differences in islet populations to quantifiable functional outcomes. The functional differences previously described between isolated large and small islets have been impressive. For example, stimulation by high glucose (20 mM), caused a release of insulin that is six times higher in the small compared to large islets.<sup>14,17</sup> Such results have been verified in human and mouse islets.<sup>15,16</sup> Other differences between the populations that we have identified suggest that isolated small islets have: (1) greater oxygen uptake, (2) better survival in culture and (3) superior diffusion properties.<sup>14</sup> However, all of these characteristics could be due to the manner in which the two populations tolerate the isolation procedures and thus could have no relevance to the *in vivo* condition.

With the work described here, we have shown that small islets have a greater cell density *in vitro* and *in situ*, and a greater insulin content *in vitro* and *in situ*. These results suggest that at least some of the functional and morphological differences noted between the large and small islets *in vitro*, are present *in vivo*. Further, the results supply the first mechanistic explanation for the differences in insulin secretion between the populations, other than large islets are more susceptible to core cell death. The concept that core cell death of large islets is responsible for all functional differences between large and small islets is no longer valid, as methods that improve the diffusion barrier of large islets reversed core cell death, but did not reverse the poor insulin secretion phenotype of the large islets.<sup>17</sup>

We tested several hypotheses to determine how small islets secreted more insulin per volume. First, we questioned whether small islets contained a greater percentage of  $\beta$ -cells compared to large islets, thus making them more efficient insulin-secretors. However, our results showed that there was no difference in the cellular composition between large and small islets *in vitro* or *in situ*. Therefore, a greater percentage of insulin-producing  $\beta$ -cells cannot explain the superior insulin secretion in small islets. Next,

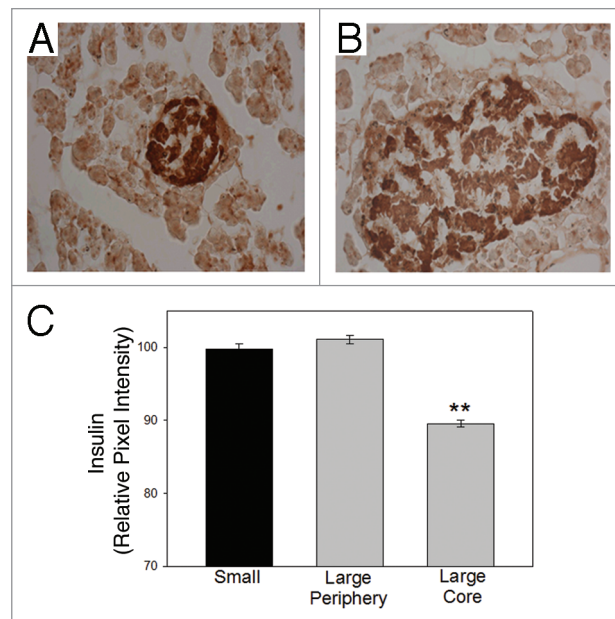


**Figure 5.** Core  $\beta$ -cells of large islets have less insulin than peripheral  $\beta$ -cells *in situ*. (A) Typical small islet showing dark insulin staining (brown) throughout the islet. (B) Typical large islet contains lighter insulin-stained  $\beta$ -cells at the core of the islet. (C) Analysis of single cells illustrates that the core  $\beta$ -cells of the large islets contain less insulin/cell. (\*\* $p < 0.001$ ).

we hypothesized that each  $\beta$ -cell within the islet was more efficient at releasing insulin. For the first time, we showed that cells of small islets contained more total insulin than cells from large islets. Thus, the two populations of islets actually secrete the same percentage of their total insulin, but cells from large islets store far less insulin to be released. More specifically, the  $\beta$ -cells found in the core of the large islets have a lower insulin content compared to the peripheral cells or the  $\beta$ -cells found in small islets. Functional differences in the core and peripheral  $\beta$ -cells has been described previously *in vivo* and *in vitro* with core  $\beta$ -cells containing fewer insulin granules after stimulation.<sup>21,27</sup>

The two most important findings were that the total number of cells per islet area was greater in small islets and the average  $\beta$ -cell contained more insulin than cells from large islets. Although the small islets account for a vast majority of the total number of islets, they make up only a very small percentage of the total islet volume. From this observation, many labs have concluded that large islets are responsible for the bulk of the pancreatic endocrine function.<sup>28,29</sup> This concept has been prevalent in the literature, with little functional data to support it. The finding that, on average, the cells of small islets contain more insulin than cells from large islets, and the *in vitro* data showing that small islets secrete significantly more insulin/volume than large islets, argues for an important role for small islets in glucose regulation *in vivo*.

It is interesting to consider the role of different islet populations during the onset and progression of type 1 and type 2 diabetes. In a rat model of type 2 diabetes (*fa/fa*) exposure of islets to high glucose was more detrimental to the  $\beta$ -cells of the

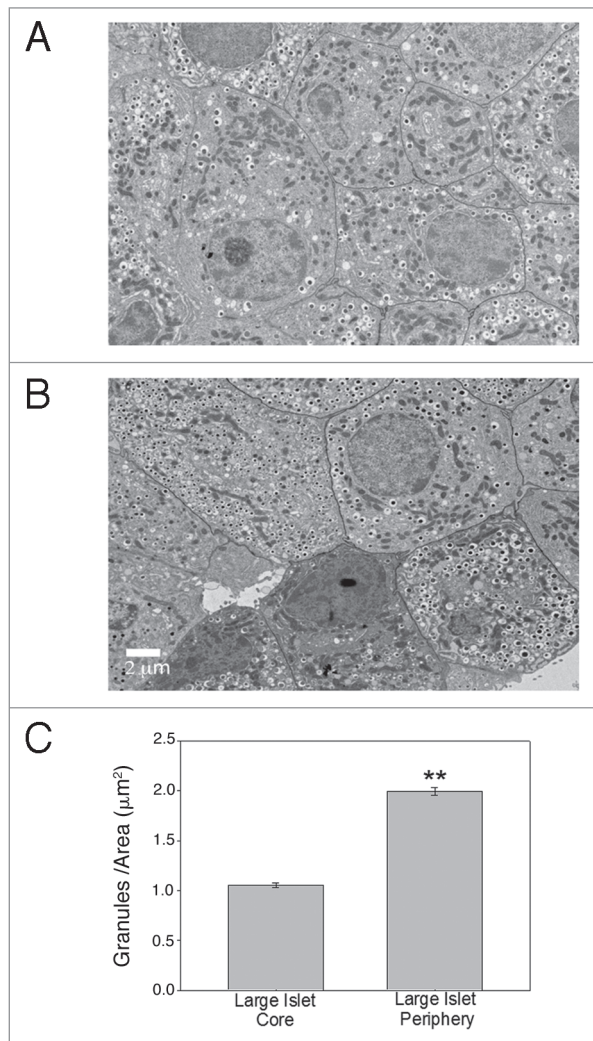


**Figure 6.** Core  $\beta$ -cells of large islets have less insulin than peripheral  $\beta$ -cells in vitro. (A) Typical  $\beta$ -cells from core of large islet with few insulin granules/area. (B) Typical  $\beta$ -cells from periphery of large islet with a higher density of insulin granules. (Scale bar = 2  $\mu\text{m}$  for both images) (C) Analysis of cells from core and periphery of large islets showed statistically greater insulin granules/area in the peripheral region. (\*\* $p < 0.001$ ).

large islets than cells from small islets.<sup>30,31</sup> These studies showed that large islets released less insulin per cell than smaller ones from the same obese animals, and significantly less than the islets from the lean animals.<sup>32</sup> Additionally, there were fewer insulin-secreting cells within the large islets of the obese rats. The authors concluded that the large islets were predominantly affected in the obese diabetic rat and that the small islets maintained normal insulin secretion during the time when the large islets had become non-functional.<sup>31,32</sup> In studies of people with type 2 diabetes, researchers noted a shift in cellular composition, with an increase in  $\alpha$ -cells and a decline in  $\beta$ -cells that was particularly noticeable in the large islets.<sup>33</sup>

The results presented here demonstrate that many of the characteristics associated with islets of different sizes after islet isolation, were consistent when examined in situ in rats.

Unique characteristics, inherent within the pancreatic tissue of rats, included a higher density of cells in the small islets with greater insulin content. Different islet populations may have important distinctions, many of which are yet to be characterized, but that may be necessary for a healthy endocrine pancreas.

## Methods

**Rat islet isolation.** Twenty-six adult, male Sprague Dawley rats (ages 7–10 weeks) were housed on a 12 hours light/dark cycle with free access to standard laboratory chow and water. All animals received care in compliance with the Principles of Laboratory Animal Care formulated by the National Society for Medical Research and the Guide for the Care and Use of Laboratory Animals published by the US National Institutes of Health (NIH Publication No. 85-23, revised 1996).

Islet isolation methods followed our published procedures described in detail.<sup>14,17,18</sup> Briefly, rats were anesthetized by intraperitoneal injection of a mixture of ketamine and xylazine. After the peritoneal cavity was exposed, the pancreatic main duct to the intestine was clamped and the pancreas cannulated in situ via the common bile duct. The pancreas was distended with collagenase and removed. Islets were gently tumbled, washed and passed through a sterile 30 mesh stainless steel screen and centrifuged. The pellet was mixed with Histopaque, centrifuged and the islets floating on the gradient were collected and sedimented. Islets were passed through a sterile 40  $\mu\text{m}$  mesh cell strainer with Hank's Buffered Salt Solution (HBSS). After this cleaning process, islets were placed into CMRL 1066 medium containing 2 mM glutamine, 10% fetal bovine serum (FBS) and 1% antibiotic/antimycotic solution and put into a 37°C culture chamber containing 5%  $\text{CO}_2$ .

Prior to experiments, the islet culture media was changed to L15 containing 10% FBS and 5 mM HEPES and islets were transferred into 37°C culture chamber without  $\text{CO}_2$ . Isolated islets were separated by size manually or by using the COPAS biosorter.<sup>17</sup> The diameter of every islet was recorded for calculating total islets volume using light microscopy. Islet Equivalents (IE) were calculated by taking duplicate samples of each batch of islets (comprising <2% of the islet fraction). Individual islets were counted and their diameters measured. For irregularly shaped islets, two to four diameter measurements were taken at different locations on the islet and averaged. Islet volumes were calculated and converted to IE for the sample and the entire islet fraction.

**Cell dispersion.** For single cell assays, intact isolated islets from eight rats were exposed to calcium-magnesium free HBSS 14.8 mM HEPES with papain (5 U/ml final concentration) using our published protocol.<sup>18</sup> After incubation on a rotator at 37°C for 30 min, the islets were pipetted, dispersing them into single cells. The cells were transferred to CMRL 1066 as the final culture medium. When necessary, islets or dispersed  $\beta$ -cells were identified with dithizone labeling following published procedures.<sup>18,19</sup>

**Tissue preparation for immunostaining.** Seven rats were anesthetized and transcardially perfused with 80–100 ml of physiological saline, followed by 250 ml of a fixative solution containing 4% paraformaldehyde in 0.1 M phosphate buffered saline

(PBS, pH 7.4) within 9 min of extermination. The pancreas was removed and dissected into three parts (head, middle and tail). Only the tail section was used for the analysis in this study.

Pancreatic samples and isolated islets were fixed in 10% normal buffered formalin in PBS, pH 7.4 for 3 days at 4°C. Paraffin embedded tissue sections were cut (7–10  $\mu\text{m}$  thickness), mounted on Superfrost/Plus microscope slides (Fisher Scientific, # 12-550-15) and dried at 40°C overnight and stored at 4°C until processing. The paraffin embedded sections were deparaffinized/rehydrated in xylene followed by ethanol and PBS serial rehydration. Antigen retrieval was completed in 0.01 M citrate buffer, pH 6.2, with 0.002 M EDTA for 30 min using a steamer. Slides were permeabilized in 1.0% Triton X-100 in 0.1 M PBS for 30 min.

**Immunofluorescence staining.** Sections from three rats (>75 islets) were blocked in 10% normal donkey serum, 1.0% bovine serum albumin (BSA) and 0.03% Triton X-100 diluted in 0.1 M PBS for 30 min. Incubation with the primary antibody mix was performed at 4°C overnight in a wet chamber followed by incubation with the mix of fluorophore conjugated secondary antibodies at room temperature for 2 hours in a wet chamber protected from light. Both primary and secondary antibodies were diluted in 1% NDS, 1% BSA and 0.03% Triton X-100. Slides were mounted with anti-fading agents. In some cases, 4',6-diamidino-2-phenylindole (DAPI, 0.5  $\mu\text{g}/\text{ml}$  Molecular Probes, # D1306) staining was performed to reveal the nuclei for 5 min at room temperature after the secondary antibody exposure.

Primary antibodies used were the following: anti-insulin (1:100, Abcam, # ab7842; 1:100, Santa Cruz Biotechnology, # sc-9168), anti-glucagon (1:200, Abcam, # ab10988) and anti-somatostatin (1:200, Abcam, # ab53165). Corresponding secondary antibodies were conjugated with Cy2 (1:200, Jackson ImmunoResearch Laboratories Inc., # 706-225-148), Alexa 647 (1:400, Molecular Probes, # A31573), Alexa 555 (1:400, Molecular Probes, # A31570) or DyLight 488 (1:400, Jackson ImmunoResearch Laboratories Inc., # 706-485-148).

Images were obtained on an Olympus Fluoview 300 confocal microscope or using a Nikon C1Si or a C1Plus confocal microscope. Images were acquired using 10x–100x objectives (depending on the experiment) and analyzed using FlouView or Ps Adobe Photoshop CZ4 software.

**Immunohistochemistry.** Insulin immunohistochemistry (IHC) was completed on pancreatic sections from four rats using anti-insulin (1:100, Santa Cruz Biotechnology, Inc., # sc-9168) and Vectastain Elite ABC kit (Vector Laboratories, #PK-6101) in combination with 3,3'-diaminobenzidine Peroxidase Substrate kit (Vector Laboratories, # SK-4100) as per manufacturer instructions. On occasions, 3-amino-9-ethyl-carbazole was used. After staining, slides were dehydrated in xylene and placed on coverslips in Permount mounting medium (Fisher Scientific, #S15-100). The specificity of insulin immunoreactivity was confirmed by omitting the primary antibodies from some sections. Images were collected on a Nikon Eclipse 80i microscope and analyzed with Ps Adobe Photoshop CZ4 extended software, by determining the average

pixel value of staining per cell or per islet. Background staining was subtracted from each value.

**Cell composition.** To determine the cell composition, the relative proportion of immuno-labeled endocrine ( $\alpha$ -,  $\beta$ - and  $\delta$ -) cells in pancreatic sections from three rats or preparations of single dispersed cells [200 cells from six rats dissociated into single cells with six aliquots of single cells from each group (small or large)] were evaluated by counting the number of individual types of cell and dividing by the total sum of endocrine cells per islet. In addition, DAPI was used to count the total cell number in the preparation.

**Islet perfusion.** Small and large islets (1,400 islets) from six rats were preincubated for 90 min in RPMI 1640 medium containing 10% FBS and 3 mM glucose at a 37°C with 5%  $\text{CO}_2$ . After preincubation, the islets were incubated in the glucose perfusion system individually with a constant flow rate (500  $\mu\text{l}/\text{min}$ ) at 37°C for 90 min including: 30 min of basal condition (3 mM glucose) following by 30 min of high glucose concentration (20 mM) and 30 min of basal condition (3 mM glucose). During the perfusion, samples of medium with released insulin were collected from the output fraction every 3 min starting with the last 10 min of the first low glucose exposure. Samples were frozen at -80°C. At the end of the perfusion, the islets were harvested and frozen at -80°C. The total protein in the islets was extracted by acid ethanol (0.18 M HCl in 95% ethanol). The released insulin and the total intracellular insulin amounts of large and small islets were determined by the ELISA (ALPCO, Salem, NH) as we have published previously in references 14, 17 and 18.

**Transmission electron microscopy.** Islets from five rats were treated with 10 nM AuNP-DNA-Cy for 24 hours, washed twice with PBS, and then transferred to fresh media containing no AuNPs for an additional 72 hours. Islets were pelleted and immersed in 2% paraformaldehyde/2.5% glutaraldehyde in 0.1 M sodium cacodylate buffer (SCB). The islets were then rinsed with 0.1 M SCB and placed in secondary fixative containing 2% osmium tetroxide in 0.1 M SCB. Next, islets were rinsed with distilled water and stained with 3% uranyl acetate. The fixed islet samples were rinsed with distilled water before undergoing a graded ethanol dehydration series. Propylene oxide was used as a transitional solvent and tissues were embedded in Embed 812 resin. Samples were placed in a 60°C oven to cure. The blocks were sectioned at the islet equatorial region using a Leica UCT ultramicrotome (80 nm thin) and then mounted on grids for imaging. Images were captured from random sections using a J.E.O.L. JEM-1400 electron microscope. Insulin granules (halo-containing granules) were counted per  $\mu\text{m}^2$  in  $\beta$ -cells from small islets (105 cells from 46 islets) and in the periphery (outer three layers) or core of large islets (155 cells from 60 islets) using standard procedures.<sup>20,21</sup> Total cell density was analyzed by counting cells within a 25 x 25  $\mu\text{m}$  region of interest in the core of each islet using published protocols at x3,800 magnification.<sup>22</sup> This method tends to overestimate the absolute cells/area, but the objective of the calculations was to compare one population of islets to another, rather than obtain an absolute value, and the approach was applied uniformly to

islets of both populations. Our published protocol was utilized to determine mitochondrial quality from final magnifications of  $\times 10,800$ .<sup>23</sup>

**Statistics.** Over 2,225 islets from 26 rats were analyzed for this study. The experimental design included comparing large and small islets from healthy animals, thus each animal provided islets for both groups. The exact number of islets/experiment is shown in the methods section. Two-Way ANOVA with Fisher Least Significant Difference (LSD) test or a Kruskal-Wallis ANOVA on Ranks was used to compare multiple groups. For the single cell assays (immunostaining and TEM

experiments) nested ANOVA was used. All figures and tables include means  $\pm$  SE.  $p$  value  $< 0.05$ , was considered statistically significant.

#### Acknowledgements

We wish to thank Ms. Barbara Fegley and Maheswari Mukherjee for assistance with TEM experiments and Karthik Ramachandran for assistance with cell density measurements. The work was funded by the Emilie Rosebud Diabetes Research Foundation and the Hall Foundation to L.S.B. Core facilities used were supported by NICHD HD02528.

#### References

- Haist R, Pugh E. Volume measurements of the Islets of Langerhans and the effects of age and fasting. *Am J Physiol* 1947; 152:36-41.
- Bonnevie-Nielsen V, Skovgaard L. Pancreatic islet volume distribution: direct measurement in preparations stained by perfusion in situ. *Acta Endocrinol (Copenh)* 1984; 105:379-84.
- Aizawa T, Kaneko T, Yamauchi K, Yajima H, Nishizawa T, Yada T, et al. Size-related and size-unrelated functional heterogeneity among pancreatic islets. *Life Sci* 2001; 69:2627-39.
- White S, Hughes D, Contractor H, London N. A comparison of cross sectional surface area densities between adult and juvenile porcine islets of Langerhans. *Horm Metab Res* 1999; 31:519-24.
- Furuzawa Y, Ohmori Y, Watanabe T. Immunohistochemical morphometry of pancreatic islets in the cat. *J Vet Med Sci* 1992; 54:1165-73.
- Elayat A, el-Naggar M, Tahir M. An immunocytochemical and morphometric study of the rat pancreatic islets. *J Anat* 1995; 186:629-37.
- Jörns A, Barklage E, Grube D. Heterogeneities of the islets in the rabbit pancreas and the problem of "paracrine" regulation of islet cells. *Anat Embryol (Berl)* 1988; 178:297-307.
- Saito K, Takahashi T, Yaginuma N, Iwama N. Islet morphometry in the diabetic pancreas of man. *J Exp Med* 1978; 125:185-97.
- Bosco D, Armanet M, Morel P, Niclauss N, Sgroi A, Muller Y, et al. Unique arrangement of  $\alpha$ - and  $\beta$ -cells in human islets of Langerhans. *Diabetes* 2010; 59:1202-10.
- Baetens D, Malaisse F, Perrelet A, Orci L. Endocrine pancreas: three-dimensional reconstruction shows two types of islets of Langerhans. *Science* 1979; 206:1323-5.
- Cabrera O, Berman D, Kenyon N, Ricordi C, Berggren PO, Caicedo A. The unique cytoarchitecture of human pancreatic islets has implications for islet cell function. *PNAS* 2006; 103:2334-9.
- Aguayo-Mazzucato C, Sanchez-Soto C, Godinez-Puig V, Gutiérrez-Ospina G, Hiriart M. Restructuring of pancreatic islets and insulin secretion in a postnatal critical window. *PLoS ONE* 2006; 35.
- Tasaka Y, Matsumoto H, Inoue Y, Hirata Y. Contents and secretion of glucagon and insulin in rat pancreatic islets from the viewpoint of the localization in the pancreas. *Tohoku J Exp Med* 1989; 159:123-30.
- MacGregor RR, Williams SJ, Tong PY, Kover K, Moore WV, Stehno-Bittel L. Small rat islets are superior to large islets in vitro function and in transplantation outcomes. *Am J Physiol Endocrinol Metab* 2006; 290:771-9.
- Lehmann R, Spinaz GA, Moritz W, Weber M. Has time come for new goals in human islet transplantation? *Am J Transplant* 2008; 8:1096-100.
- Su Z, Xia J, Shao W, Cui Y, Tai S, Ekberg H, et al. Small islets are essential for successful intraportal transplantation in a diabetes mouse model. *Scand J Immunol* 2010; 72:504-10.
- Williams S, Huang HH, Kover K, Moore W, Berkland C, Singh M, et al. Reduction of diffusion barriers in isolated islets improves survival, but not insulin secretion. *Organogenesis* 2010; 6:115-24.
- Williams S, Wang Q, MacGregor R, Siahaan T, Stehno-Bittel L, Berkland C. Adhesion of pancreatic beta cells to biopolymer films. *Biopolymers* 2009; 91:676-85.
- Mythili D, Patra S, Gunasekaran S. Culture prior to transplantation preserves the ultrastructural integrity of monkey pancreatic islets. *J Electron Microscop* 2003; 52:399-405.
- Pisania A, Weir G, O'Neil J, Omer A, Tchivashvili V, Lei J, et al. Quantitative analysis of cell composition and purity of human pancreatic islet preparations. *Lab Invest* 2010; 90:1661-75.
- Stefan Y, Meda P, Neufeld M, Orci L. Stimulation of insulin secretion reveals heterogeneity of pancreatic B cells in vivo. *J Clin Invest* 1987; 80:175-83.
- Obermuller S, Calegari F, King A, Lindqvist A, Lundquist I, Salehi A, et al. Defective secretion of islet hormones in chromogranin-B deficient mice. *PLoS ONE* 2010; 5:8936.
- Searls Y, Smirnova I, Fegley B, Stehno-Bittel L. Exercise attenuates diabetes-induced ultrastructural changes in rat cardiac tissue. *Med Sci Sports Exerc* 2004; 36:1863-70.
- Morini S, Braun M, Onori P, Cicalese L, Elias G, Gaudio E, et al. Morphological changes of isolated rat pancreatic islets: a structural, ultrastructural and morphometric study. *J Anat* 2006; 209:381-92.
- el-Naggar M, Elayat A, Ardawi M, Tahir M. Isolated pancreatic islets of the rat: an immunohistochemical and morphometric study. *Anat Rec* 1993; 237:489-97.
- Yorde D, Kalkhoff R. Quantitative morphometric studies of pancreatic islets obtained from tolbutamide-treated rats. *J Histochem Cytochem* 1986; 34:1195-2000.
- Salomon D, Meda P. Heterogeneity and contact-dependent regulation of hormone secretion by individual B cells. *Exp Cell Res* 1986; 162:507-20.
- Kaihoh T, Masuda T, Sasano N, Takahashi T. The size and number of Langerhans islets correlated with their endocrine function: a morphometry on immunostained serial sections of adult human pancreases. *Tohoku J Exp Med* 1986; 149:1-10.
- Hellman B. The volumetric distribution of pancreatic islet tissue in young and old rats. *Acta Endocrinologica* 1959; 31:91-106.
- Chan C, Saleh M, Purje A, MacPhail R. Glucose-inducible hypertrophy and suppression of anion efflux in rat beta cells. *J Endo* 2002; 173:45-52.
- Chan C, Surette J. Glucose refractoriness of cells from fed fa/fa rats is ameliorated by nonesterified fatty acids. *Can J Physiol Pharmacol* 1999; 77:934-42.
- Chan C, Wright G, Wadowska D, MacPhail R, Ireland W, Sulston K. Ultrastructural and secretory heterogeneity of fa/fa (Zucker) rat islets. *Mol Cell Endocrinol* 1998; 136:119-29.
- Yoon K, Ko S, Cho J, Lee J, Ahn Y, Song K, et al. Selective  $\beta$ -cell loss and  $\alpha$ -cell expansion in patients with type 2 diabetes mellitus in Korea. *J Clin Endocrinol Metab* 2003; 88:2300-8.